

The Importance of Grain Boundaries for the Time-Dependent Mobility Degradation in Organic Thin-Film Transistors

R. T. Weitz,^{*,†} K. Amsharov,[†] U. Zschieschang,[†] M. Burghard,[†] M. Jansen,[†] M. Kelsch,[‡] B. Rhamati,[‡] P. A. van Aken,[‡] K. Kern,^{†,§} and H. Klauk[†]

[†]Max Planck Institute for Solid State Research, Heisenbergstrasse 1, 70569 Stuttgart, Germany,

[‡]Max Planck Institute for Metals Research, Heisenbergstrasse 3, 70569 Stuttgart, Germany, and [§]Institut de Physique de la Matière Condensée, Ecole Polytechnique Fédérale de Lausanne, 1015 Lausanne, Switzerland

Received July 15, 2009. Revised Manuscript Received August 19, 2009

The relationships between organic semiconductor morphology and device stability of organic field-effect transistors (FETs) are very complex and not yet fully understood. Especially for obtaining high-performance, air-stable n-channel FETs, gaining a deep insight into possible degradation mechanisms can help improve their air stability. Here, we investigate the performance and stability of organic n-channel FETs based on solution-grown single-crystalline ribbons of the conjugated semiconductor bis(1*H*,1*H*-perfluorobutyl)-dicyano-terylene tetracarboxylic diimide (C₃F₇CH₂–PTCDI–(CN)₂). The FETs show an electron mobility of 0.25 cm²/(V s) in air and an on/off ratio up to 1 × 10⁷. Their mobility does not significantly change when devices are stored in air for more than 5 weeks. This excellent air stability stands in contrast to FETs based on thin evaporated polycrystalline films of the same compound that degrade by more than an order of magnitude during the same 5 week period. We attribute this striking difference in air stability to the grain boundaries in the polycrystalline films and discuss different possible degradation mechanisms.

Introduction

The charge carrier mobility in organic field-effect transistors (FETs) is greatly influenced by the microstructure of the organic semiconductor.^{1–3} For example, the mobility in pentacene FETs can be as high as 35 cm²/(V s) if the semiconductor is a single-crystal,⁴ but less than 7 cm²/(V s) if it is a polycrystalline film.^{5,6} This difference is related to grain boundaries and other defects that act as scattering sites for the charge carriers in polycrystalline films.² For practical applications, not only the absolute value of the mobility but also its stability under ambient conditions is important. Although the stability of organic FETs in the presence of oxygen and humidity has been

studied extensively,^{7–9} no coherent picture of the relationships between microstructure and environmental stability has been established yet.

Here we show how the microstructure of bis(1*H*,1*H*-perfluorobutyl)-dicyano-terylene tetracarboxylic diimide (C₃F₇CH₂–PTCDI–(CN)₂; molecular structure shown in the inset to Figure 1)^{10–12} affects the rate at which the mobility of n-channel FETs based on this semiconductor degrades over time while exposed to ambient air. The reason for choosing a PTCDI derivative as the semiconductor for this study is that these molecules have a high degree of chemical inertness.¹³ This eliminates the oxidation of the conjugated molecules as a possible cause for the mobility degradation and allows us to focus on other mechanisms, such as changes in the crystal structure due to the incorporation of ambient species (water, oxygen, nitrogen) into the semiconductor.^{7,8} This is an advantage over previous mobility degradation studies that utilized organic molecules with greater susceptibility to oxidation, most notably pentacene.^{14,15}

*Corresponding author. Present address: Department of Physics, Harvard University, Cambridge, MA 02138. E-mail: tweit@physics.harvard.edu.

- (1) Gundlach, D. J.; Lin, Y. Y.; Jackson, T. N.; Nelson, S. F.; Schlom, D. G. *IEEE Electron. Dev. Lett.* **1997**, *18*, 87.
- (2) Mas-Torrent, M.; Hadley, P.; Bromley, S. T.; Ribas, X.; Tarres, J.; Mas, M.; Molins, E.; Veciana, J.; Rovira, C. *J. Am. Chem. Soc.* **2004**, *126*, 8546.
- (3) Weitz, R. T.; Amsharov, K.; Zschieschang, U.; Villas, E. B.; Goswami, D. K.; Burghard, M.; Dosch, H.; Jansen, M.; Kern, K.; Klauk, H. *J. Am. Chem. Soc.* **2008**, *130*, 4637.
- (4) Jurchescu, O. D.; Popinciuc, M.; van Wees, B. J.; Palstra, T. T. M. *Adv. Mater.* **2007**, *19*, 688.
- (5) Lee, S.; Koo, B.; Shin, J.; Lee, E.; Park, H.; Kim, H. *Appl. Phys. Lett.* **2006**, *88*, 162109.
- (6) Choi, C. G.; Baez, B. S. *Electrochem. Solid-State Lett.* **2007**, *10*, H347.
- (7) Northrup, J. E.; Chabiny, M. L. *Phys. Rev. B* **2003**, *68*, 041202.
- (8) De Angelis, F.; Cipolloni, S.; Mariucci, L.; Fortunato, G. *Appl. Phys. Lett.* **2006**, *88*, 193508.
- (9) Klauk, H.; Zschieschang, U.; Weitz, R. T.; Meng, H.; Sun, F.; Nunes, G.; Keys, D. E.; Fincher, C. R.; Xiang, Z. *Adv. Mater.* **2007**, *19*, 3882.

- (10) Jones, B. A.; Ahrens, M. J.; Yoon, M. H.; Facchetti, A.; Marks, T. J.; Wasielewski, M. R. *Angew. Chem., Int. Ed.* **2004**, *43*, 6363.
- (11) Jones, B. A.; Facchetti, A.; Wasielewski, M. R.; Marks, T. J. *J. Am. Chem. Soc.* **2007**, *129*, 15259.
- (12) Jones, B. A.; Facchetti, A.; Wasielewski, M. R.; Marks, T. J. *Adv. Funct. Mater.* **2008**, *18*, 1329.
- (13) Würthner, F. *Chem. Commun.* **2004**, 1564.
- (14) Vollmer, A.; Jurchescu, O. D.; Arfaoui, I.; Salzmann, I.; Palstra, T. T. M.; Rudolf, P.; Niemax, J.; Pflaum, J.; Rabe, J. P.; Koch, N. *Eur. Phys. J. E* **2005**, *17*, 339.
- (15) Kalb, W. L.; Mattenberger, K.; Batlogg, B. *Phys. Rev. B* **2008**, *78*, 035334.

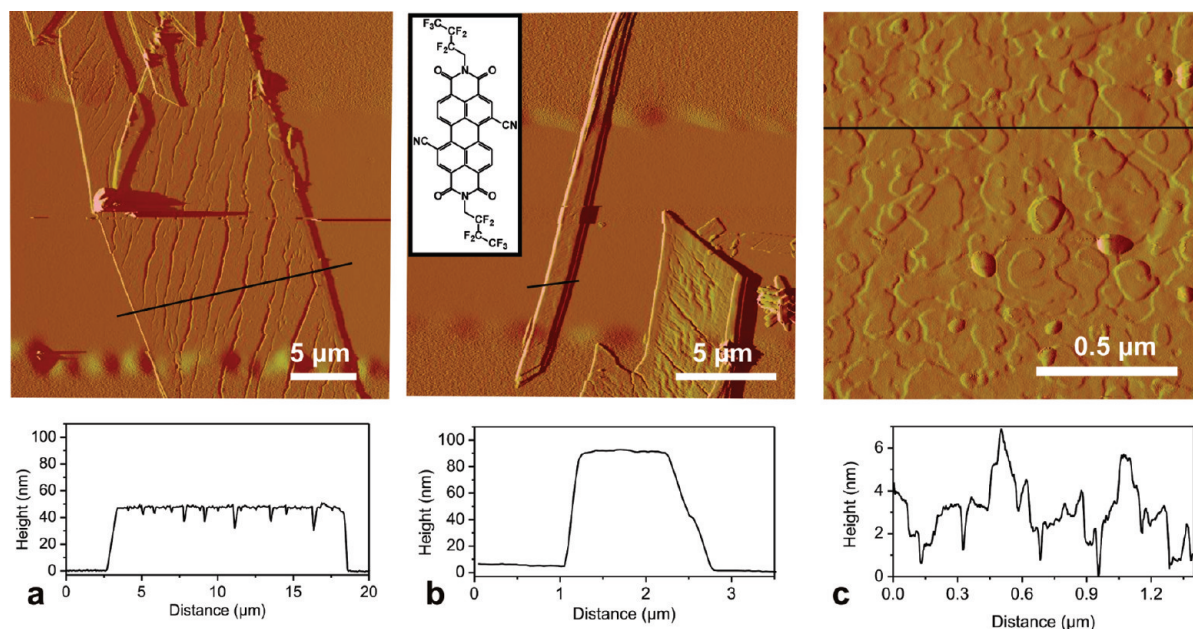


Figure 1. (a, b) Atomic force microscopy (AFM) amplitude images of two solution-grown $\text{C}_3\text{F}_7\text{CH}_2\text{-PTCDI-(CN)}_2$ ribbons, with 200 nm thick Au top contacts deposited by evaporation through a shadow mask. (c) AFM amplitude image of a vacuum-deposited 30 nm thick $\text{C}_3\text{F}_7\text{CH}_2\text{-PTCDI-(CN)}_2$ film. During the vacuum deposition, the substrate was held at a temperature of 120 °C. (The black line in each image indicates the position at which the line scan shown underneath each AFM image was taken.) Inset: Molecular structure of $\text{C}_3\text{F}_7\text{CH}_2\text{-PTCDI-(CN)}_2$.

To investigate the relationship between the $\text{C}_3\text{F}_7\text{CH}_2\text{-PTCDI-(CN)}_2$ microstructure and the stability of the electron mobility, we have fabricated FETs based on polycrystalline $\text{C}_3\text{F}_7\text{CH}_2\text{-PTCDI-(CN)}_2$ films prepared by vacuum deposition, as well as FETs based on $\text{C}_3\text{F}_7\text{CH}_2\text{-PTCDI-(CN)}_2$ single-crystals grown from solution at room temperature. To the best of our knowledge, this is the first report of $\text{C}_3\text{F}_7\text{CH}_2\text{-PTCDI-(CN)}_2$ single-crystals obtained by a solution-based method.

Experimental Section

The single-crystals were prepared using the procedure reported by Briseno et al.¹⁶ A saturated solution of $\text{C}_3\text{F}_7\text{CH}_2\text{-PTCDI-(CN)}_2$ in trichloromethane (~ 1.5 mg/mL) was injected to the bottom of a beaker filled with methanol (in which $\text{C}_3\text{F}_7\text{CH}_2\text{-PTCDI-(CN)}_2$ is insoluble). Ribbon-shaped, micrometer-sized $\text{C}_3\text{F}_7\text{CH}_2\text{-PTCDI-(CN)}_2$ crystals with a thickness of 50–100 nm formed within a few hours as a result of the supersaturation of the trichloromethane solution, caused by the slow interdiffusion of the two solvents. The ribbons were collected with a pipet and drop-cast onto degenerately doped, thermally oxidized silicon wafers functionalized with a hydrophobic self-assembled monolayer of octadecyltrichlorosilane (OTS). The doped Si substrate serves as the gate electrode and the 100 nm thick SiO_2 layer as the gate dielectric. The OTS monolayer reduces the defect density at the dielectric/semiconductor interface. Ribbon FETs were completed by evaporating gold source and drain contacts with a thickness of 200 nm through a shadow mask, giving a channel length of 10 or 20 μm . The channel width of the ribbon FETs is identical to the width of the $\text{C}_3\text{F}_7\text{CH}_2\text{-PTCDI-(CN)}_2$ crystals, which was determined for each device by optical microscopy.

FETs based on polycrystalline $\text{C}_3\text{F}_7\text{CH}_2\text{-PTCDI-(CN)}_2$ films were prepared as described previously.³ In brief, a doped Si wafer with a SiO_2 gate dielectric (100 nm thick) functionalized with an OTS monolayer served as the substrate and gate electrode. Thirty-nanometer-thick films of $\text{C}_3\text{F}_7\text{CH}_2\text{-PTCDI-(CN)}_2$ were deposited by sublimation in vacuum. During the vacuum deposition, the substrates were held at a temperature of 120 °C, since this has been shown to promote the growth of continuous, polycrystalline films.³ Gold source and drain contacts were evaporated through a shadow mask, giving a channel length of 100 μm . The electrical measurements on both the ribbon FETs and the thin-film FETs were performed in ambient air at room temperature under yellow laboratory light.

Results and Discussion

The atomic force microscopy (AFM) images a and b in Figure 1 suggest the existence of two different ribbon morphologies. Ribbon A (Figure 1a) is 15 μm wide and 50 nm high, and thus has a relatively large aspect ratio of 300. In contrast, ribbon B (Figure 1b) is only 1.5 μm wide, but 90 nm tall, and thus has a much smaller aspect ratio of 17. A second notable difference is that the surface of ribbon A shows numerous cracks, whereas the surface of ribbon B appears to be continuous. For comparison, Figure 1c shows an AFM image of a $\text{C}_3\text{F}_7\text{CH}_2\text{-PTCDI-(CN)}_2$ film obtained by vacuum deposition with a substrate temperature of 120 °C. The average film thickness is 30 nm. X-ray diffraction measurements confirm that the film is polycrystalline,³ with an average grain size of about 100 nm.

To investigate the crystallinity of the solution-grown ribbons, we have performed transmission electron microscopy (TEM) using selected-area electron diffraction (SAED) on both types of ribbon. The TEM images in

(16) Briseno, A. L.; Mannsfeld, S. C. B.; Reese, C.; Hancock, J. M.; Xiong, Y.; Jenekhe, S. A.; Bao, Z.; Xia, Y. *Nano Lett.* **2007**, 7, 2847.

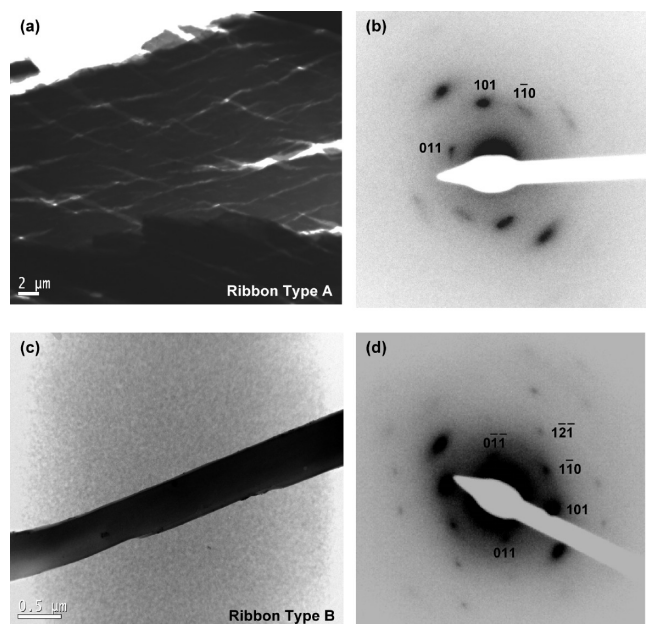


Figure 2. (a, c) Bright-field transmission electron microscope (TEM) images of two solution-grown $\text{C}_3\text{F}_7\text{CH}_2\text{-PTCDI-(CN)}_2$ ribbons. (b, d) Selected-area electron diffraction (SAED) patterns of the same ribbons. Diffraction spots are indexed with the Miller indices (hkl) of the corresponding lattice plane distances using the lattice parameters reported by Jones et al.¹⁰ Both diffraction patterns have the zone axis $[\bar{1}\bar{1}\bar{1}]$.

Figure 2a and c confirm the observation made by AFM regarding the difference in surface roughness between the two types of ribbon. SAED patterns recorded in various positions along each ribbon are essentially identical, indicating that both types of ribbon are single-crystalline. Unfortunately, the ribbons are very unstable when exposed to the electron beam and become amorphous after a few seconds of irradiation, which is why the reflections in the SAED patterns are smeared out (see Figure 2b). Using the unit cell dimensions reported by Jones et al. (triclinic, $P\bar{1}$, $Z = 1$, $a = 5.2320(14)$ Å, $b = 7.638(2)$ Å, $c = 18.819(5)$ Å; $\alpha = 92.512(5)^\circ$, $\beta = 95.247(5)^\circ$, $\gamma = 104.730(4)^\circ$, $V = 722.5(3)$ Å³),¹⁰ we were able to assign the SAED diffraction spots of both types of ribbon to lattice planes (hkl), as shown in Figure 2b and d. The common zone axis for both diffraction patterns is the $[\bar{1}\bar{1}\bar{1}]$ direction. The growth direction of the ribbons was found to be the $[110]$ direction.

We have measured the current–voltage characteristics of about 20 ribbon-based FETs. The electron mobility extracted from the transfer curves (I_D versus V_{GS}) ranges from $0.001 \text{ cm}^2/(\text{V s})$ to $0.25 \text{ cm}^2/(\text{V s})$. Since the extracted mobilities were not corrected for contact resistance,¹⁷ we cannot determine whether this significant variation is due to variations in intrinsic mobility or variations in contact resistance. The current–voltage characteristics of the two FETs with the largest mobilities are shown in Figure 3; these are the FETs that were made from ribbon A (AFM image in Figure 1a) and ribbon B (Figure 1b). The FET based on ribbon A has an electron mobility of $0.25 \text{ cm}^2/(\text{V s})$

(V s) and an on/off ratio of 1×10^7 (see Figure 3a). The transistor based on ribbon B has a mobility of $0.21 \text{ cm}^2/(\text{V s})$ and an on/off ratio of 1×10^4 (see Figure 3b).

The largest mobility we have measured for vacuum-deposited $\text{C}_3\text{F}_7\text{CH}_2\text{-PTCDI-(CN)}_2$ FETs immediately after fabrication is about $0.1 \text{ cm}^2/(\text{V s})$, and these transistors have an on/off ratio of $1 \times 10^{5.3}$. The fact that the maximum mobility of the thin-film FETs is smaller than the maximum mobility of the ribbon FETs is likely related to the significant density of grain boundaries in the vacuum-deposited polycrystalline films that act as scattering and/or trapping sites for the charge carriers.^{18,19}

Although this is the first report of solution-grown $\text{C}_3\text{F}_7\text{CH}_2\text{-PTCDI-(CN)}_2$ ribbons, there are several studies in which this semiconductor was used to make FETs using other fabrication techniques.^{10–12,20,21} Comparing the performance of these devices we find that the mobility of our solution-grown $\text{C}_3\text{F}_7\text{CH}_2\text{-PTCDI-(CN)}_2$ ribbons is smaller than the mobility reported by Jones et al. for FETs based on vacuum-deposited thin films of the same material ($0.64 \text{ cm}^2/(\text{V s})$),¹⁰ and smaller than the mobility reported by Molinari et al. for FETs based on $\text{C}_3\text{F}_7\text{CH}_2\text{-PTCDI-(CN)}_2$ crystals grown by physical vapor transport (3 to $6 \text{ cm}^2/(\text{V s})$).²⁰ But the on/off ratio of our FET based on ribbon A (10^7) is substantially larger than the on/off ratios reported by either Jones or Molinari for FETs measured in air (1×10^3 to 1×10^4). Interestingly, Jones et al. also reported an on/off ratio of 10^7 for an FET based on a vacuum-deposited $\text{C}_3\text{F}_7\text{CH}_2\text{-PTCDI-(CN)}_2$ film,¹² but that FET was characterized in vacuum, and the mobility was smaller ($0.15 \text{ cm}^2/(\text{V s})$). Recently, Piliego et al. prepared $\text{C}_3\text{F}_7\text{CH}_2\text{-PTCDI-(CN)}_2$ FETs by spin-coating and measured an electron mobility of $0.15 \text{ cm}^2/(\text{V s})$ in vacuum, but the leakage current at negative gate-source voltage was substantial ($> 1 \mu\text{A}$) and the on/off ratio was no greater than 1×10^4 .²¹

The electrical characteristics of our FETs were measured every few days while the substrates were stored in ambient air at room temperature for five weeks. Figure 4 shows the evolution of the mobility and threshold voltage of the two ribbon-based FETs and the polycrystalline thin-film FET from Figure 1. The mobility of ribbon A remained essentially constant and the mobility of ribbon B decreased by a factor of 2 over the 5 week period. The mobility evolution was independent of whether the FETs were stored in the dark (first 31 days) or under ambient light (after day 31; hatched regions in panels a and b in Figure 4). The observation that the mobility in ribbon A is stable and the mobility in ribbon B degrades slightly may be related to the different surface roughness, as discussed above. In contrast to the single-crystalline ribbons, the mobility of the vacuum-deposited films degrades far more rapidly, by

(17) Takeya, J.; Yamagishi, M.; Tominari, Y.; Hirahara, R.; Nakazawa, Y.; Nishikawa, T.; Kawase, T.; Shimoda, T.; Ogawa, S. *Appl. Phys. Lett.* **2007**, *90*, 102120.

(18) Nelson, S. F.; Lin, Y. Y.; Gundlach, D. J.; Jackson, T. N. *Appl. Phys. Lett.* **1998**, *72*, 1854.

(19) Kelley, T. W.; Frisbie, C. D. *J. Phys. Chem. B* **2001**, *105*, 4538.

(20) Molinari, A. S.; Alves, H.; Chen, Z.; Facchetti, A.; Morpurgo, A. F. *J. Am. Chem. Soc.* **2009**, *131*, 2462.

(21) Piliego, C.; Jarzab, D.; Gigli, G.; Chen, Z.; Facchetti, A.; Loi, M. A. *Adv. Mater.* **2009**, *21*, 1573.

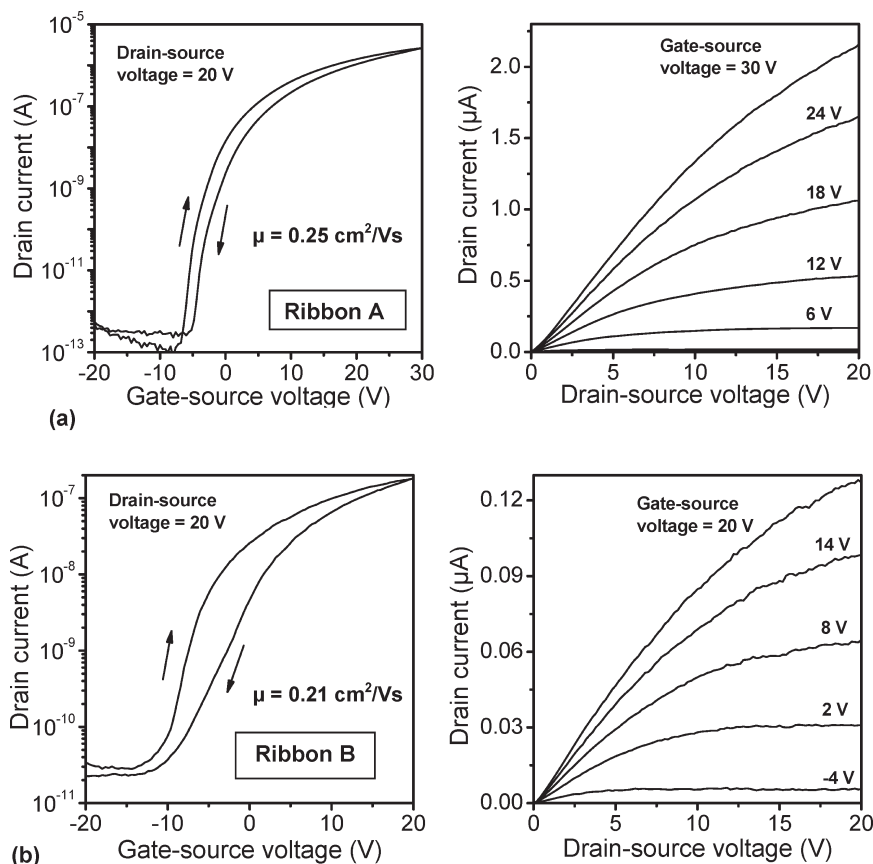


Figure 3. Electrical characteristics of the two solution-grown $\text{C}_3\text{F}_7\text{CH}_2\text{-PTCDI-(CN)}_2$ ribbon-based FETs from Figure 1.

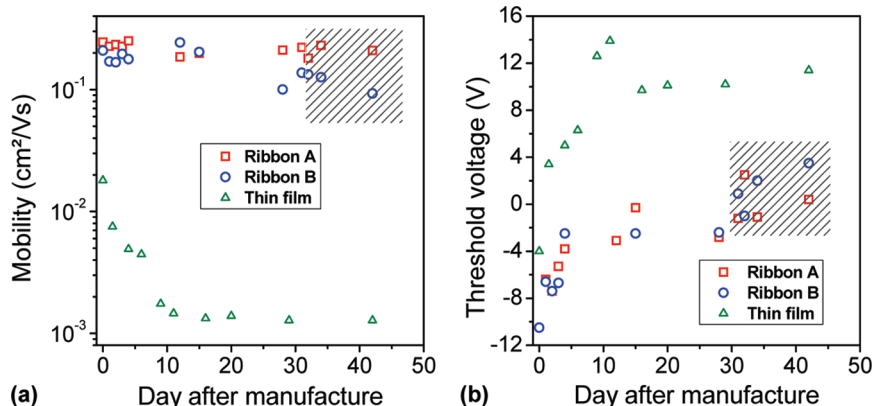


Figure 4. Evolution of (a) electron mobility and (b) threshold voltage of the two solution-grown $\text{C}_3\text{F}_7\text{CH}_2\text{-PTCDI-(CN)}_2$ ribbon-based FETs from Figure 1 and a vacuum-deposited polycrystalline $\text{C}_3\text{F}_7\text{CH}_2\text{-PTCDI-(CN)}_2$ thin-film FET over a period of 5 weeks while being stored in ambient air. During the first 31 days, the ribbon-based FETs were stored in the dark; after that, they were kept under ambient light (hatched regions).

more than an order of magnitude over the same 5 week period. As we have previously reported,³ vacuum-deposited $\text{C}_3\text{F}_7\text{CH}_2\text{-PTCDI-(CN)}_2$ films are either polycrystalline or amorphous, depending on the substrate temperature during the deposition, and the polycrystalline films have much larger mobility ($> 1 \times 10^{-2} \text{ cm}^2/(\text{V s})$) than the disordered films ($< 1 \times 10^{-3} \text{ cm}^2/(\text{V s})$). In the same report we showed that the mobility in the vacuum-deposited $\text{C}_3\text{F}_7\text{CH}_2\text{-PTCDI-(CN)}_2$ films degrades with the same rate, regardless of whether the films are polycrystalline or amorphous, and regardless of the orientation of the $\text{C}_3\text{F}_7\text{CH}_2\text{-PTCDI-(CN)}_2$ molecules with respect to the substrate surface. This observation is consistent with the

recent report by Piliego et al. who showed that the mobility of spin-coated $\text{C}_3\text{F}_7\text{CH}_2\text{-PTCDI-F(CN)}_2$ films also degrades over time,²¹ similar to our vacuum-deposited films.³

Figure 4a shows that the mobility in $\text{C}_3\text{F}_7\text{CH}_2\text{-PTCDI-(CN)}_2$ FETs exposed to air evolves quite differently, depending on whether the semiconductor is a single-crystalline ribbon or a polycrystalline or disordered film. While the mobility in the ribbons is essentially constant over 35 days, the mobility in the films degrades by an order of magnitude. This result appears to be in conflict with our previous study³ where we showed that the mobility decay rate in vacuum-deposited $\text{C}_3\text{F}_7\text{CH}_2\text{-PTCDI-(CN)}_2$ films exposed to air is independent of the

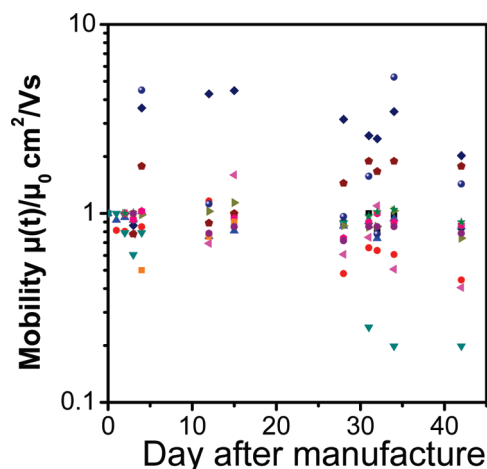


Figure 5. Evolution of the electron mobility of 13 solution-grown $\text{C}_3\text{F}_7\text{CH}_2\text{-PTCDI-F(CN)}_2$ ribbon-based FETs fabricated on the same substrate over a period of five weeks in ambient air. All mobilities were normalized to the mobility measured immediately after fabrication to facilitate better comparison across all 13 FETs.

grain boundary density. However, it is evident that the difference between the solution-grown ribbons and the vacuum-deposited films in terms of their density of grain boundaries is much larger than the variations in grain boundary density among the vacuum-deposited films. All the vacuum-deposited films³ have a density of grain boundaries that is much greater than in the single-crystalline ribbons. We believe the presence of grain boundaries in the polycrystalline films substantially accelerates the time-dependent degradation of the carrier mobility during air exposure. A similar conclusion was drawn by Li et al. from experiments on FETs based on vacuum-deposited polycrystalline pentacene films exposed to humid nitrogen.²²

Figure 5 summarizes the evolution of the mobility of 13 solution-grown $\text{C}_3\text{F}_7\text{CH}_2\text{-PTCDI-(CN)}_2$ ribbons on the same substrate while exposed to ambient air. In most of the transistors the mobility does not change substantially from its initial value over 6 weeks. In three transistors, the mobility initially increases slightly, whereas in one transistor, the mobility drops by a factor of 5 over 6 weeks. Despite these device-to-device variations, it is clear that the mobility of the ribbon-based FETs degrades far less rapidly than the mobility of the polycrystalline films.

In addition to the electron mobility, we have also monitored the evolution of the threshold voltage over time. Figure 4b shows that the threshold voltage of the solution-grown ribbon-based FETs shifts by approximately 10 V during the 5 weeks of air exposure, from initially negative values (about -8 V) to slightly positive values (about $+2$ V), while the threshold voltage of the vacuum-deposited thin-film FETs shifts by approximately 15 V (from about -4 V to about $+11$ V). Although the microscopic origin of the threshold voltage shift is unclear, it appears to be the result of p-doping of the semiconductor. Because the threshold voltage shift in the solution-grown ribbon-based FETs is smaller than in

the vacuum-deposited thin-film FETs, it appears that the solution-grown ribbons are less susceptible to the diffusion of ambient species into the semiconductor than the vacuum-deposited films.

The observation that in the polycrystalline films both the mobility and the threshold voltage change over time, while in the ribbons only the threshold voltage changes, but the mobility remains essentially constant for five weeks, indicates that different mechanisms are responsible for the mobility degradation and the threshold voltage shift. A possible explanation is that some of the ambient species interact with the channel in the ribbon-based FETs (causing a threshold voltage shift) without affecting the mobility.

Regarding the microscopic mechanism by which the grain boundaries promote the mobility degradation during air exposure, we assume that the chemical composition of the conjugated molecules does not change over time, i.e., the $\text{C}_3\text{F}_7\text{CH}_2\text{-PTCDI-(CN)}_2$ molecules are not oxidized.¹³ On this basis, a possible mechanism for the mobility degradation observed in polycrystalline $\text{C}_3\text{F}_7\text{CH}_2\text{-PTCDI-(CN)}_2$ films is an air-induced reorientation of the molecules, i.e., slight changes in the crystal structure over time. It has been shown that distorted or displaced molecules form charge traps that impede the drift of electrons through the film by reducing the amount of overlap between the delocalized molecular orbitals of neighboring molecules, and thereby reduce the carrier mobility.²³ Molecules located at grain boundaries are expected to be particularly susceptible to reorientations, because they are usually undercoordinated (i.e., they have fewer neighbors than molecules inside of the grains). In polycrystalline films with many grain boundaries, the number of reorientation events will thus be substantial, and these reorientations will significantly increase the number of trapping events as charge carriers traverse the grain boundaries. In other words, with time, the grain boundaries become less and less transparent to carrier transport. In contrast, the solution-grown ribbons are essentially free of grain boundaries, so reorientation events will occur only at the air-exposed surfaces of the ribbons, with negligible impact on the carrier transport (which occurs in a thin conduction channel near the gate dielectric interface).

There appear to be two possible microscopic mechanisms for the reorientation of organic molecules at grain boundaries. One mechanism is the diffusion of small inorganic molecules, such as N_2 , O_2 , or H_2O , from the ambient air into the organic film. The intercalation of these molecules in the semiconductor will cause a distortion of the surrounding lattice and thereby introduce scattering defects. This has been theoretically predicted for pentacene²⁴ and is likely to occur in polycrystalline films of $\text{C}_3\text{F}_7\text{CH}_2\text{-PTCDI-(CN)}_2$ as well. Another mechanism is the redistribution or relaxation of conjugated molecules (especially those at the grain boundaries) to a thermodynamically more stable configuration that may

(22) Li, D. W.; Borkent, E. J.; Nortrup, R.; Moon, H.; Katz, H.; Bao, Z. N. *Appl. Phys. Lett.* **2005**, *86*, 042105.

(23) Anthony, J. E. *Angew. Chem., Int. Ed.* **2008**, *47*, 452.

(24) Tsetseris, L.; Pantelides, S. T. *Phys. Rev. B* **2007**, *75*, 153202.

be characterized by larger intermolecular distances and hence smaller carrier mobility. This mechanism appears quite plausible, because vacuum-deposited organic semiconductor films do not usually grow in thermodynamic equilibrium.

In contrast to the vacuum-deposited films, the ribbons grow in thermodynamic equilibrium and are therefore essentially free of grain boundaries, so that the incorporation of ambient molecules into the crystal and the redistribution of conjugated molecules will be restricted to the surfaces and edges of the ribbons, where the effect on the transport properties is negligible.

Conclusion

In summary, we have investigated the performance and stability of the electron mobility and threshold

voltage of organic n-channel FETs from solution-grown single-crystalline ribbons of the conjugated semiconductor $\text{C}_3\text{F}_7\text{CH}_2\text{-PTCDI-F(CN)}_2$. Measured in ambient air, the ribbon FETs have an electron mobility up to $0.25 \text{ cm}^2/(\text{V s})$ and an on/off ratio up to 1×10^7 . The mobility is essentially constant when the devices are stored in ambient air for more than five weeks. The excellent air stability of the $\text{C}_3\text{F}_7\text{CH}_2\text{-PTCDI-(CN)}_2$ single crystals is in contrast to the characteristics of vacuum-deposited polycrystalline thin films of the same semiconductors, the mobility of which degrades by more than an order of magnitude during the same 5 week period. This significant difference in air stability suggests that the grain boundaries in the polycrystalline film are responsible for the mobility degradation.